Improving automated global detection of volcanic SO₂ plumes using the Ozone Monitoring Instrument (OMI)

Verity J. B. Flower, Thomas Oommen, Simon A. Carn

Dept. Geological and Mining Engineering and Sciences, Michigan Technological University, 1400 Townsend Dr, Houghton,

5   MI 49931, USA

Correspondence to: Verity J. B. Flower (vjflower@mtu.edu)

Abstract. Volcanic eruptions pose an ever-present threat to human populations around the globe, but many active volcanoes remain poorly monitored. In regions where ground-based monitoring is present the effects of volcanic eruptions can be

10   moderated through observational alerts to both local populations and service providers such as air traffic control. However, in regions where volcano monitoring is limited satellite-based remote sensing provides a global data source that can be utilised to provide near real time identification of volcanic activity. This paper details the development of an automated volcanic plume detection method utilizing daily, global observations of sulphur dioxide (SO_2) by the Ozone Monitoring Instrument (OMI) on NASA's Aura satellite. Following identification and classification of known volcanic eruptions in 2005-2009, the OMI SO_2

15   data are analysed using a logistic regression analysis which permits the identification of volcanic events with an overall accuracy of over 80%, and consistent plume identification when the volcanic plume SO_2 loading exceeds ~400 tons. The accuracy and minimal user input requirements of the developed procedure provide a basis for the creation of an automated SO_2 alert system providing volcanic alerts in regions where ground based volcano monitoring capabilities are limited. The technique could easily be adapted for use with satellite measurements of volcanic SO_2 emissions from other platforms.

20   **1 Introduction**

Volcanic eruptions pose a global hazard due to the potential for emissions to be entrained into the upper atmosphere and transported globally. The addition of these particles can result in significant impacts locally as fine particulate matter in the atmosphere can cause significant health problems (Delmelle et al., 2002, Hansell & Oppenheimer, 2004) and impacts to the aviation industry (Miller & Casadevall, 1999; Prata, 2009) in addition to alterations to the radiative transfer rates through the

25   atmosphere on a global scale as seen following the eruption of Mt Pinatubo (Self et al., 1993), in order to mitigate the possible impacts of volcanic eruptions timely warning of events are essential. The installation of a global network of ground-based monitoring stations would be both costly and impractical however satellite-based monitoring provides the spatial and temporal coverage necessary to facilitate the near-real time (NRT) monitoring of global volcanism (Brenot et al., 2014). Existing techniques employ a threshold approach in order to identify volcanic eruptions however this limits the capabilities in regards

30   to smaller events and can be susceptible to the effect of high background noise levels. The following work outlines a method

for the identification of volcanic plumes utilising a background correction factor. The resulting output was processed with a binary classification algorithm in order to identify the strength of the developed methodology to distinguish volcano events from control samples.

The Ozone Monitoring Instrument (OMI), launched on NASA's Aura satellite in July 2004, provides near global daily

5   monitoring of multiple atmospheric trace gases with absorption bands in the ultraviolet (UV) spectral band, and was designed to supersede the Total Ozone Monitoring Spectrometer (TOMS) instrument. Due to its strong absorption bands in the UV, sulphur dioxide (SO_2) can be discerned by instruments designed to measure ozone (Krueger, 1983). The ability of satellite-based ozone monitoring instrumentation to detect and monitor volcanic SO_2 emissions was first demonstrated by the identification of the eruption plume of El Chichón in 1982 (Krueger, 1983), which led to the implementation of satellite based

10 UV measurements as a volcano monitoring tool (Schneider et al., 1999; Krueger et al., 2008). The low spatial resolution of the TOMS instruments precluded the measurement of SO_2 in all but the largest volcanic eruptions (Carn et al., 2003), but OMI's higher spatial resolution (13 x 24 km at nadir) permits detection of smaller eruptions and passive volcanic degassing of SO_2, whilst providing daily global coverage (Krotkov et al., 2006; Carn et al., 2013, 2016). This work utilises the continuous global coverage of OMI to identify and automatically classify volcanic eruption events based on common characteristics.

15 **1.1 Existing alert systems**

An operational alert system known as the Support to Aviation Control Service (SACS) is currently employed in the assessment of SO_2 and ash emitted from volcanoes (Brenot et al., 2012). This service provides near real time (NRT) alerts of anomalously high SO_2 amounts and ash indices recorded by three UV instruments; OMI and Global Ozone Monitoring Experiment-2 (GOME-2; maintained on-board two meteorological satellites MetOp-A and MetOp-B) and three infrared (IR) instruments;

20 the Atmospheric Infrared Sounder (AIRS) and Infrared Atmospheric Sounding Interferometer (IASI; also flown on the MetOp-A and B platforms). The method of SO_2 alert generation used by SACS (Brenot et al. 2014; http://sacs.aeronomie.be/info/index.php) involves the initial identification of an anomalously high SO_2 column amount (>2 DU). When a pixel is flagged the area is analysed in greater detail and an alert is only generated if more than half of the neighbouring pixels also display high SO_2 values (>2 DU). The technique developed by Brenot et al. (2014) is subject to

25 certain limitations when utilising UV data including; the systematic noise in the data leading to false alerts and the restriction of retrievals to those that assume a SO_2 plume altitude in the lower stratosphere (STL). Therefore, in the development of an algorithm based on OMI data we aim to account for variable background SO_2 levels and systematic noise, in addition to using SO_2 retrievals assuming a lower plume altitude in an attempt to resolve plumes with lower SO_2 amounts, lower injection altitude and more diffuse characteristics.

Atmospheric
Measurement
Techniques
Open Access
Discussions
EGU

2 Methodology

2.1 Data collection

OMI Level 2 total column SO_2 (OMSO2) data are publicly available from NASA Goddard Earth Sciences (GES) Data and Information Services Center (DISC; http://disc.sci.gsfc.nasa.gov/Aura/data-holdings/OMI/omso2_v003.shtml). These data

5   provide global coverage with a temporal resolution of 1 day at low latitudes and increasing daily observations towards the poles, where measurement swaths overlap. OMSO2 data currently provide volcanic SO_2 total column amounts calculated using a linear fit (LF) algorithm (Yang et al., 2007) for three distinct layers of the atmosphere; corresponding to centre of mass altitudes (CMA) of approximately 3 km (lower troposphere; TRL), 8 km (mid-troposphere; TRM) and 17 km (lower stratosphere; STL). These altitudes are based upon atmospheric pressure levels and therefore can display slight variations

10 depending upon the local conditions such as temperature profile (Carn et al., 2013). In order to obtain an accurate estimation of the SO_2 column amount the appropriate retrieval must be selected based upon the known or inferred injection altitude of the volcanic plume (Yang et al., 2007), which can be poorly constrained particularly in remote regions with minimal or no monitoring capabilities (Sparks, 2012). Differences between the altitude assumed in the LF algorithm and the true altitude of the plume can lead to errors of up to 20%, provided the assumption is approximately correct (Yang et al., 2007). Due to the

15 focus of this work on a variety of plumes displaying diverse eruptive characteristics, we use SO_2 data from the TRL OMSO2 product in order to facilitate identification of eruptions confined to the lower troposphere. The use of one retrieval altitude reduces the need for user input or prior knowledge of the injection altitude of the plume however results in the overestimation of plume mass for features injected above the retrieval altitude therefore this method is for identification and alert purposes as opposed to accurate plume mass calculation. Previous works have provided in depth descriptions of the OMI retrieval

20 algorithms (Carn et al., 2013; Krotkov et al., 2006; McCormick et al., 2013; Yang et al., 2007) with a proven track record in the assessment of volcanic and anthropogenic emissions including identification of volcanic plume sources (e.g., Carn et al., 2008; McCormick et al., 2012; Carn et al., 2013, 2016; McCormick et al., 2013), volcanic plume tracking (e.g., Carn and Prata 2010; Krotkov et al., 2010; Lopez et al., 2013) and identification of copper smelter emissions (Carn et al., 2007) and other large SO_2 emission sources (e.g., Fioletov et al., 2011, 2013).

25 OMI data collected since 2008 are influenced by a row anomaly (the OMI row anomaly; ORA) which results in data gaps in particular rows along the OMI measurement swath. Information on the status of this anomaly is provided by the Royal Netherlands Meteorological Institute (www.knmi.nl/omi/). The ORA data gaps combined with the variation in viewing angle produced by the 16-day orbital cycle of the Aura satellite results in varying influence on OMI SO_2 measurements (Flower et al., 2016). Any eruptions identified after the formation of the ORA were investigated with greater scrutiny and excluded where

30 the effect was significant.

Atmospheric
Measurement
Techniques
Discussions
Open Access
EGU

2.2 Volcanic plume quantification

As a test dataset for our plume identification technique, we identified 79 volcanic eruptions at 27 different volcanoes (Table 1) using the Volcanoes of the World (VOTW) database curated by the Smithsonian Institution's Global Volcanism Program (GVP; http://volcano.si.edu/). Note that, as a result of the way in which eruptions are defined in the VOTW database, several

5   of the eruptions listed in Table 1 actually correspond to the onset of extended periods of volcanic activity, rather than discrete eruptions. For each identified eruption, total SO_2 mass detected by OMI was obtained for the registered day of the eruptive event (or the start of the period of unrest) with the preceding and subsequent days analysed where no corresponding plume could be identified on the reported day of eruption. This allowance accounts for any inaccuracies in the assigned eruption date, and allows for the identification of eruption plumes generated after the Aura overpass time (~1345 local time) resulting in a

10   delay in detection. Identification and quantification of volcanic SO_2 emissions is complicated by the presence of variable biases and noise levels in the data. These variations are influenced by several factors including the latitude of the volcano, time of year, proximity to pollution sources, and the presence of meteorological clouds (Krotkov et al., 2006; Yang et al., 2007).

In our analysis, three methods (M1, M2, and M3; Table 1) were used to quantify the SO_2 loading detected at each location, with the goal of distinguishing volcanic SO_2 from background noise. The procedures were developed with the intention of

15   allowing the calculation of volcanic SO_2 loading with minimal user input, reducing the possible effects of human error in the classification of what constitutes the bounds of an identified plume.

Method 1 (M1) and Method (M2) differ only in the geographic extent over which OMI SO_2 columns are integrated to obtain total SO_2 mass (Fig. 1). For each eruption analysed, M1 calculates integrated SO_2 mass in a 4°×4° box centred over the volcano location (thus capturing plumes regardless of wind direction). The 4°×4° box encompasses an area which captures most small-

20   moderate volcanic plumes with few instances of dispersion of emissions outside the region; however, this relatively large sample area also potentially includes increased background noise, which could generate false alerts in locations with higher noise levels. As an alternative to M1, M2 uses a 2°×2° region which, whilst more susceptible to possible plume dispersion beyond the defined limits, is less influenced by noise contamination (Fig. 1). Manual inspection indicated that plume dispersion beyond the defined geographic limits was only an issue for the largest eruptions in Table 2. Figure 1 shows an example of a

25   small volcanic SO_2 plume at Piton de la Fournaise volcano (Réunion); here, the M2 region captures most of the SO_2 plume that is visually apparent, only excluding some very diffuse SO_2 further downwind that is included in the M1 region.

A third method (M3) was developed in an attempt to intrinsically account for the variable noise levels in SO_2 data collected in different geographic regions (Carn et al. 2013). We posit that in order to effectively develop a volcanic plume detection methodology without a significant number of false alerts a background noise correction may be necessary. Our technique is

30   analogous to contextual thermal infrared (TIR) anomaly detection procedures used at active volcanoes, where a background radiance value is calculated as a reference against which anomalously high radiance values can be compared (e.g., Wright et al. 2002; Murphy et al., 2011). In the M3 method, the 2°×2° region (M2) is considered the active emission region with a background SO_2 offset value derived from the total SO_2 mass in the 4°×4° M1 region (Eq. 1).

$$M3 = M2 - \frac{M1 - M2}{3} \tag{1}$$

Eruptive events that post-date the appearance of the ORA were manually assessed in order to identify whether the ORA data gap significantly impacted the detection of SO_2, such as complete masking of the plume in extreme cases (Flower et al., *in prep*). Additional factors impacting the selection of eruptive events are the presence of meteorological clouds, which can
5   effectively mask any volcanic plume at lower altitudes from a satellite-based sensor (Carn et al., 2013; Krotkov et al., 2006), and the seasonal variation in UV radiation at high latitudes. Cloud masking is due to the high UV albedo of clouds and this, coupled with low UV irradiance, can make SO_2 detection at high latitudes during winter months particularly challenging (Telling et al., 2015). Hence the majority of the eruptions analysed here are located at latitudes below 30°.

2.3 Control samples

10   A control group is required to assess whether volcanic eruptions can be distinguished from background SO_2 levels. Therefore, for each volcanic eruption analysed (Table 2) a control SO_2 mass was calculated using each of the three incorporated methodologies (M1, M2 and M3) for a second date at the same volcano. Assignment of control group analysis dates was limited to a period between 1st January 2005 and 31st December 2009. The 2009 cut-off date was employed due to the increasing influence of the ORA after this time, in an attempt to reduce the influence of data gaps on the model output. Control dates
15   were assigned for comparison with each identified volcanic eruption, using an online random number generator (Haahr, 2015; *http://www. random.org*) to assign a value between 0 and 1825 to each data point. These random values were used to determine the number days from the beginning of the analysis period at which to assign a control date (Table 2). The identified dates were then assigned to each target volcano alphabetically, with a corresponding number of events assigned to each location as number of volcanic eruption analyses performed (Table 2).

20   **2.4 Modelling techniques**

Modelling procedures were conducted with the Weka 3 software package; a collection of algorithms that can be implemented for data mining tasks (Hall et al., 2009) provided by the University of Waikato (http://www.cs.waikato.ac.nz/ml/weka/). Significant differences in measured SO_2 mass were found between the samples due to variations in eruption magnitude, background noise levels and SO_2 emission strength displayed by the incorporated volcanoes preventing the calculation of a
25   flat emission threshold for the classification of the eruptive events.
Within the Weka 3 package, a simple logistic regression analysis (Eq. 2) was found to be an effective technique for the classification of volcanic and non-volcanic events. Simple logistic regression is a binary classification technique, here defining volcanic (*v*) and non-volcanic control (*c*) events facilitating the development of a linear model constructed from a transformed target variable (Witten & Frank, 2005). The logistic regression equation used here assigns the probability *P* of the occurrence
30   of a volcanic eruption or degassing event;

$$P = 1 - \frac{1}{1 + e^{-(a + bX)}}, \tag{2}$$

Atmospheric
Measurement
Techniques
Discussions

where e is the base of the natural logarithm, a is the probability when the independent variable (X) is equal to zero, and b represents the rate at which probabilities vary with incremental changes in X, which in this case is the volcanic plume SO_2 mass measured in tons.

Output of a logistic regression analysis is assessed against a series of validation statistics that test the accuracy of the generated model. These statistics include overall accuracy, precision and recall, in addition to Receiver Operating Characteristic (ROC) curves. In this analysis, the overall accuracy relates to the percentage of c,orrectly classified events in both the volcanic and control (non-volcanic) samples; however, this statistic alone cannot account for preferential classification of one sample over another (Oommen et al. 2010). Hence precision and recall statistics, characterised by values between 0 and 1, are incorporated in order to identify whether preferential classification is occurring. Precision relates to the accuracy of prediction of a single sample group (volcanic or non-volcanic) whilst recall measures the effectiveness of the predictions themselves (Oommen, et al. 2010). In the context of this study, if a volcanic classification has a precision of 0.9, then 90% of the events predicted as being volcanic in nature are volcanic events, whilst the remaining 10% are misclassified as non-volcanic and will be termed here as 'missed alerts'. In contrast, a recall value of 0.8 would correspond to 80% of observed volcanic events being correctly classified, but this does not take into account any non-volcanic events which are misclassified as volcanic, referred to here as 'false alerts'. The final validation statistic used here is the ROC curve, which represents a method for assessing the rate of accurately classified events against possible falsely classified events. ROC values relate to the accuracy of the classification system implemented with a value of 1 indicating accurate prediction of all events (Oommen et al., 2010; Witten & Frank, 2005).

Logistic regression model calculation was conducted using the k-fold cross validation technique incorporated into the Weka 3 software package. This method segregates the data into k partitions, allowing k-1 folds of the data to be used as a training set with the remaining data used for validation purposes. This method is then repeated with each of the k partitions being used to validate the corresponding model from which it was withheld, with the final statistics comprising an average of the output of all k models (Oommen et al. 2010). We implement a k value of 10 due to the associated reduction in bias compared to k values <5 (Rodríguez et al., 2010; Witten & Frank, 2005).

3 Results

3.1 OMI SO₂ measurements

Of the 79 volcanic eruptions analysed, 13 displayed low SO_2 amounts (<100 tons), following application of the SO_2 correction (M3), on the identified day of eruption. Two eruptions produced very large amounts of SO_2: Nyamuragira (Nov 2006; 46 kt) and Rabaul (Oct 2006; 550 kt), although use of the OMI TRL SO_2 columns is likely to overestimate the actual SO_2 amounts in these upper tropospheric or lower stratospheric plumes (Carn et al., 2013).

Excluding the aforementioned very high values, the average M3 plume contained 680 t SO_2, approximately 60% of the average of the M2 analysis and 25% of the M1 average (Table 3). The control dataset displays significantly lower SO_2 loadings than

the volcanic events with an average corrected SO_2 mass of 90 t and a maximum corrected SO_2 mass of 1040 t. This variation indicates that the volcanic data displays generally higher SO_2 levels than the control data, as would be expected. In all of the selection methodologies the SO_2 mass detected on control dates was 14-17% of the average mass detected in the volcanic dataset. Box plots were generated to assess the general dynamics of the volcanic and control datasets (Fig. 2). Comparison of these plots confirms the pattern identified in Table 3, with the SO_2 measurements on 'eruption' days displaying significantly higher values than the control data.

3.2 Initial review

Of the three SO_2 mass calculation procedures employed (M1, M2 and M3), the most success was achieved with the background-corrected dataset (M3). None of the logistic regression model investigations undertaken with the M1 and M2 datasets produced more than 55% overall accuracy in the classification of volcanic events, and therefore these data were not investigated further. However, the M3 technique provided the best results with a 77% overall accuracy, with no additional data pre-processing required, therefore this technique was employed for all further assessments and model development.

3.3 Model output

The most accurate model consisted of a simple logistic regression applied to the M3 SO_2 dataset with an overall accuracy of 76.6% and an ROC of 0.843. This model favoured volcanic precision (volcanic precision of 0.83 vs control of 0.72) at the expense of control recall (control recall of 0.86 vs volcanic of 0.67), which indicates that the model preferentially classifies alerts as control samples, therefore reducing the number of false alerts generated relative to missed alerts. Investigations were undertaken to identify characteristics of volcanic events that facilitated classification and to elucidate the likely cause of the 23% error associated with the model.

Removal of volcanic plumes containing less than 50 t SO_2 from the M3 dataset resulted in a ~6% increase in model accuracy. Eight data points produced false alerts with control events classified as volcanic eruptions, whilst 18 volcanic events were misclassified as controls, producing missed alerts (Table 4). The misclassified alerts were isolated to assess if any common characteristics of these events could be identified, with each individual alerts incorporated into Figure 2 for comparison with the overall dynamics of the data. The comparison of missed alerts indicates that each one falls within the lower quartile of the volcanic dataset, whilst the false alerts displayed values consistent with the upper quartile of the control data range (with one exception; Fig. 2). The potential causes of the misclassification of events are discussed further in section 4.1.

Atmospheric
Measurement
Techniques
Discussions

4 Discussion

4.1 Analysis of inaccurate classifications

4.1.1 False alerts

Investigation of the incorrectly classified false alerts (Fig. 2; Table 4) revealed that, due to the random selection procedure
used for assigning control sample dates, some of the control SO_2 values corresponded to periods of ongoing volcanic activity.
These anomalous control values relate to stronger, persistent plumes, despite not being associated with large or 'initiating'
events as reported in the VOTW database; this was the case for five of the nine false alerts (C1, 8, 32, 54 and 57; Table 4).
Two additional alerts were generated as a result of a data gap in the OMI measurements (C10 and 24); this indicates that
missing values (characterised by a blank cell to differentiate these from days with data available but no recordable SO_2
emissions) are likely to be incorrectly classified by the incorporated model as volcanic events and therefore screening of
samples for data gaps prior to incorporation into the model is required to prevent the classification of missing values as volcanic
events. The one remaining false alert (C29) was the result of increased noise levels preferentially affecting the M2 over the
M1 region, resulting in an artificially high SO_2 mass derived from the M3 calculation and a false alert.

4.1.2 Missed alerts

Missed alerts occurred at a higher frequency than false alerts, but a common characteristic of all missed alerts is an SO_2 plume
mass below 325 t (Fig. 2; Table 4). We attribute the misclassification of volcanic events to four main causes. The first
influenced eight of the volcanic events (V3, 13, 20, 23, 28, 32, 33 and 48; Table 4) and is the result of eruptions producing
diffuse plumes containing low SO_2 amounts close to the OMI detection limit (e.g., small eruptions and/or eruptions to low
altitudes). The second cause of misclassification affecting eight samples (V5, 17, 21, 24, 34, 43, 64 and 67; Table 4) is the
drifting of the volcanic plume out of the geographic area of analysis (M2) into the region utilised for background classification
(M1), causing signal suppression in the M3 methodology. One event (V19; Table 4) was impacted by increased noise in the
background classification region, also suppressing the plume SO_2 loading in the M3 calculation. The final factor preventing
the correct identification of a volcanic eruption (V53; Table 4) occurred at Popocatepetl (Mexico), through the masking of a
moderate eruption plume when a large SO_2 cloud from another volcano (Soufriere Hills, Montserrat) drifted into the M1 region
causing an anomalously high background SO_2 mass in the M3 calculation.

4.2 Optimisation of event classification

We assessed the impact of varying the maximum SO_2 plume mass included in the logistic regression model, to investigate
whether the use of a threshold SO_2 loading improved the classification capabilities of the model. The volcanic dataset was
incrementally filtered to remove a proportion of the data, to identify how this influenced the validation statistics. Each reduced
volcanic dataset was incorporated into a logistical regression model with a k-fold validation system; however, the control
sample was maintained throughout all of the analyses. The variation in class size produced by the removal of volcanic data

actually provides a more accurate representation of the natural system (Oommen et al. 2011), with more control samples than volcanic, as more days are characterised by quiescence than volcanic activity. In each instance the overall accuracy, precision and recall statistics were tracked (Fig. 3) to assess the changes in the model as the minimum incorporated SO_2 mass varied. The linear correlation between control recall and volcanic precision is evident in the comparison of these statistics (Fig. 3b) as well as that between the control precision and volcanic recall.

When all data are incorporated, the model appears to favour volcanic precision and control recall resulting in a model that will display a larger number of missed volcanic alerts than false classification of control samples. When 60% of the dataset is used, the volcanic precision and recall are equal as are the control precision and recall, all displaying values greater than 0.9. The threshold SO_2 loading in this case is 360 tons, i.e., if this model were to be implemented any volcanic plume containing less than 360 tons of SO_2 would not be identified as a volcanic event. The use of 75% of the volcanic dataset appears to represents a good compromise between variation in the statistics and the elimination of smaller plumes (Fig. 3). The volcanic and control precision are almost equal, indicating that this model is equally effective at predicting volcanic and non-volcanic events respectively, with a higher control recall than volcanic recall (Fig. 3) indicating the tendency of the model to miss smaller volcanic events rather than falsely classify control samples displaying moderate noise levels as volcanic eruptions. Favouring missed over false alerts is a characteristic of the MODVOLC automatic volcanic alert system designed to detect volcanic thermal anomalies (Wright et al., 2002, 2004). Comparison of these models could not be conducted as assessment of the MODVOLC system was performed in a qualitative manner, assessing whether alerts were identified in locations where they would be expected (e.g. lava flow fields).

Figure 4 shows the variation of ROC values associated with each of the logistic regression models and minimum SO_2 plume mass with the percentage of the total dataset analysed, with the total change in each normalised. The trends in both ROC and SO_2 mass threshold show 2nd order polynomial characteristics with R^2 values of 0.985 and 0.993, respectively. The intersection of these trend lines represents model optimisation, offering the greatest gain in accuracy (ROC) combined with the least impact on the identifiable SO_2 plume mass. This optimisation point corresponds to the removal of 22% of the volcanic data, resulting in a minimum incorporated SO_2 mass of ~150 t and correlates with that inferred through the comparison of precision and recall statistics (Fig. 3). Application of a 150 t SO_2 mass threshold prevents the resolution of smaller plumes, but the original assessment (Fig. 2; Table 4) indicates that SO_2 loadings below this value tended to be misclassified anyway.

The model based on 78% of the volcanic dataset has an overall accuracy of 85.7% and an ROC of 0.95, producing 8 false alerts that correspond to those identified in the original assessment, with the exception of C8 (Table 4) which was accurately classified with this model. In contrast, 27.8% of the missed alerts originally identified were no longer flagged; of these five instances, four were eliminated due to their low SO_2 loadings with the remaining alert correctly classified as a result of improvements in event classification by the optimised model.

Parameterization of Equation 2 using the 78% model output facilitates the validation of individual records and allows the incorporation of new data points (Eq. 3) through the substitution of X with measured volcanic SO_2 mass in tons:

Atmospheric
Measurement
Techniques
Open Access
EGU
Discussions

$$P = 1 - \frac{1}{1+e^{-(-2.943+0.0091X)}}, \tag{3}$$

4.3 Independent validation

A secondary testing procedure was employed to assess the efficacy of the developed logistic regression models on an independent test dataset consisting of 12 volcanic eruptions (Global Volcanism Program, 2013) not initially identified and displaying variable plume characteristics, and 12 corresponding control samples resulting in 24 data points (Table 5).

5

The incorporation of an independent investigation allowed the data characteristics isolated in the original analysis to be tested against data not utilised in the training of the model. Classification of the data with the original model containing all data points resulted in an accuracy of 75%, whereas analysis with the optimised model (78% of the data) produced an overall accuracy of 79.2%; a detailed overview of the validation statistics of each model is given in Table 6. The optimised model resulted in no

10

false detections although four volcanic events were missed; these consisted of one sample in which the SO_2 plume had drifted out of the analysis area (Soufriere Hills), two weak plumes with SO_2 loadings below 60 tons (Cleveland & Lascar) and one moderate plume with SO_2 loadings of 255 t (Colima). All SO_2 plumes exceeding 390 t were correctly classified as volcanic, therefore we conclude that events emitting less than 390 t SO_2 are likely to be misclassified with this methodology. Taking into account the thresholds of the incorporated methods (Table 6) and solving Eq. 3, we find that the minimum SO_2 mass that

15

would be classified as volcanic in origin by this model is 378 t.

4.4 Limitation

This analysis has indicated that prior to implementation of the incorporated classification technique (logistic regression), pre-screening of data samples is required to account for the influence of missing data points and meteorological cloud cover. The incorporated modelling technique automatically interpreted missing values as volcanic alerts subsequently influencing the alert

20

threshold and therefore data gaps must be removed prior to linear regression analysis. Persistent meteorological cloud cover can mask SO_2 plumes at lower altitudes from satellite sensors, precluding detection. This effect can be significant at higher latitudes, particularly in winter, and therefore the methodology described here may be limited in these locations. Where high latitude data were available and incorporated into this trial (Bezymianny, Okmok and Cleveland) correct classification occurred in all but one of those days where data was available (one additional control sample characterised by no available data was

25

misclassified) indicating the robust nature of the M3 pre-processing technique employed, however further investigation is required to accurately assess the capabilities in high latitude regions particularly regarding the influence of persistent cloud cover.

The main constraint on SO_2 plume detection using this methodology is the detection limit of the satellite measurements used as input (here, the OMI TRL SO_2 columns). Indeed, this analysis indicates that the minimum SO_2 mass that could be reliably

30

classified as volcanic in origin using the OMI TRL SO_2 data is on the order of 400 tons. The lack of a-priori knowledge of volcanic SO_2 plume altitude restricts the classification technique to SO_2 retrievals corresponding to a single CMA, and our use

of the TRL SO_2 product does not imply any knowledge of SO_2 altitude (which is not required for eruption detection). However, the use of OMI SO_2 products with lower noise (e.g., STL columns) or more sensitive SO_2 algorithms (e.g., Li et al., 2013) should result in lower detection limits. Furthermore, future UV satellite instruments such as the Tropospheric Monitoring Instrument (TROPOMI; http://www.tropomi.eu/), with better spatial resolution than OMI, should also have lower SO_2

5 detection limits. Another limitation of this methodology relates to issues in the original data, in particular those restricting the minimum plume that can be resolved. This factor is related to the spatial resolution of the original data which cannot be overcome through processing techniques. In order to resolve smaller plumes an instrument with a higher spatial resolution would be required however existing higher resolution instruments sacrifice temporal resolution in order to facilitate the identification of small features and therefore do not provide the daily coverage necessary in the creation of a global near real

10 time alert system.

5 Conclusion

Through the analysis of operational OMI SO_2 measurements (TRL SO_2 columns) for 79 volcanic eruptions, a simple logistic regression model allowed classification of volcanic from non-volcanic control events with an accuracy of 80%. Optimisation of the model by progressive removal of input data enabled volcanic plumes containing at least 400 tons of SO_2 to be

15 consistently resolved and correctly classified. With an appropriate training dataset, this technique could form the basis of a near real-time volcanic eruption detection scheme, with minimal user input necessary. Individual assessment of specific regions could provide more accurate plume classification, however this would require a significant number of eruptions to facilitate training of the data and therefore would only be feasible where persistently degassing volcanoes are present such as Vanuatu or Indonesia.

20 We identified some common factors resulting in misclassification of control or volcanic events, including; contamination of the background analysis region with SO_2 emissions from a separate volcano; low SO_2 emissions and/or low plume altitude (i.e., resulting in emissions below detection limits); advection of SO_2 emissions out of the analysis region prior to the satellite overpass; and data gaps.

The implementation of a NRT volcanic eruption alert system based on the technique described here would represent an advance

25 over current systems, such as SACS, which use a simple threshold SO_2 column amount to identify significant volcanic degassing events (Brenot et al, 2014). In dispersed volcanic clouds, SO_2 column amounts may be low yet the total SO_2 loading could be high; hence alerts based on SO_2 mass rather than column amount may be more effective in certain situations. However, techniques based on a threshold SO_2 column amount would be more effective at identifying drifting volcanic clouds far from the source, since a reference background region is not required and elevated SO_2 amounts may be detected regardless of

30 location. Hence some combination of both approaches would likely yield an optimal NRT volcanic cloud detection system. For example, drifting volcanic clouds could be located based on elevated SO_2 column amounts, with SO_2 loading then quantified using the approach described here.

Atmospheric
Measurement
Techniques
Discussions

Data availability

OMI Level 2 total column SO$_2$ (OMSO2) data are publicly available from NASA Goddard Earth Sciences (GES) Data and Information Services Center (DISC; http://disc.sci.gsfc.nasa.gov/Aura/data-holdings/OMI/omso2_v003.shtml). The OMI processing code used to analyse this data (OMIplot) is available from the Vhub website (https://vhub.org/resources/682).

5 **Acknowledgements**

References

Brenot, H., Theys, N., Clarisse, L., Van Geffen, J. H., Van Gent, J., Van Roozendael, M., van der A, R., Coheur, P.-F.,
10 Clerbaux, C., Valks, P., Hedelt, P., Prata, F., Rasson, O., Sievers, K., & Zehner, C. (2014). Support to Aviation Control Service (SACS): an online service for near-real-time satellite monitoring of volcanic plumes. Natural hazards and earth system sciences, 14(5), 1099-1123.

Carn, S.A., L. Clarisse and A.J. Prata (2016), Multi-decadal satellite measurements of global volcanic degassing, J. Volcanol. Geotherm. Res., 311, 99-134, http://dx.doi.org/10.1016/j.jvolgeores.2016.01.002.

15 Carn, S. A., Krotkov, N. A., Yang, K., & Krueger, A. J. (2013). Measuring global volcanic degassing with the Ozone Monitoring Instrument (OMI). Geological Society, London, Special Publications, 380(1), 229-257. doi:10.1144/SP380.12.

Carn, S.A., A.J. Krueger, N.A. Krotkov, S. Arellano, and K. Yang (2008). Daily monitoring of Ecuadorian volcanic degassing from space, J. Volcanol. Geotherm. Res., 176(1), 141-150, doi:10.1016/j.jvolgeores.2008.01.029.

Carn, S. A., Krueger, A. J., Bluth, G. J. S., Schaefer, S. J., Krotkov, N. A., Watson, I. M., & Datta, S. (2003). Volcanic eruption
20 detection by the Total Ozone Mapping Spectrometer (TOMS) instruments: A 22-year record of sulphur dioxide and ash emissions. Geological Society, London, Special Publications, 213(1), 177-202.

Carn, S. A., Krueger, A. J., Krotkov, N. A., Yang, K., & Levelt, P. F. (2007). Sulfur dioxide emissions from Peruvian copper smelters detected by the Ozone Monitoring Instrument. Geophysical Research Letters, 34(9).

Carn, S. A., & Prata, F. J. (2010). Satellite-based constraints on explosive SO2 release from Soufrière Hills Volcano,
25 Montserrat. Geophysical Research Letters, 37(19).Delmelle, P., Stix, J., Baxter, P., Garcia-Alvarez, J., & Barquero, J. (2002). Atmospheric dispersion, environmental effects and potential health hazard associated with the low-altitude gas plume of Masaya volcano, Nicaragua. Bulletin of Volcanology, 64(6), 423-434.

Fioletov, V. E., C. A. McLinden, N. Krotkov, M. D. Moran, and K. Yang (2011), Estimation of SO$_2$ emissions using OMI retrievals, Geophys. Res. Lett., 38, L21811, doi:10.1029/2011GL049402.

Atmospheric
Measurement
Techniques
Discussions

Fioletov, V. E., et al. (2013), Application of OMI, SCIAMACHY, and GOME-2 satellite SO_2 retrievals for detection of large emission sources, J. Geophys. Res. Atmos., 118, doi:10.1002/jgrd.50826.

Flower, V.J.B., Carn, S.A., (2015). Characterising volcanic cycles at Soufriere Hills Volcano, Montserrat: time series analysis of multi-parameter satellite data. Journal of Volcanology and Geothermal Research.

5   Flower, V.J.B., Carn, S.A., & Wright, R., (2016). Impacts of sensor viewing geometry on time-series analysis of volcanic emissions. Remote Sensing of Environment. doi: 10.1016/j.rse.2016.05.022

Global Volcanism Program, 2013. Volcanoes of the World, v. 4.4.3. Venzke, E (ed.). Smithsonian Institution. Downloaded 11 Jun 2016. http://dx.doi.org/10.5479/si.GVP.VOTW4-2013

Haahr, M. (2015). Random.org: True random number service. School of Computer Science and Statistics, Trinity College,
10   Dublin, Ireland. Website (http://www. random. org). Accessed, June 2015.

Hall, M., Frank, E., Holmes, G., Pfahringer, B., Reutemann, P., & Witten, I. H. (2009). The WEKA data mining software: an update. ACM SIGKDD explorations newsletter, 11(1), 10-18

Krotkov, N. A., Carn, S. A., Krueger, A. J., Bhartia, P. K., & Yang, K. (2006). Band residual difference algorithm for retrieval of SO 2 from the Aura Ozone Monitoring Instrument (OMI). Geoscience and Remote Sensing, IEEE Transactions on, 44(5),
15   1259-1266.

Krotkov, N.A., M.R. Schoeberl, G.A. Morris, S.A. Carn, and K. Yang (2010). Dispersion and lifetime of the SO_2 cloud from the August 2008 Kasatochi eruption, J. Geophys. Res., 115, D00L20, doi:10.1029/2010JD013984.

Krueger, A. J. (1983). Sighting of El Chichon sulfur dioxide clouds with the Nimbus 7 total ozone mapping spectrometer. Science, 220(4604), 1377-1379.

20   Krueger, A., Krotkov, N., & Carn, S. (2008). El Chichon: The genesis of volcanic sulfur dioxide monitoring from space. Journal of Volcanology and Geothermal Research, 175(4), 408-414.

Li, C., J. Joiner, N. A. Krotkov, and P. K. Bhartia (2013), A fast and sensitive new satellite SO_2 retrieval algorithm based on principal component analysis: Application to the ozone monitoring instrument, Geophys. Res. Lett., 40, doi:10.1002/2013GL058134.

25   Lopez, T., Carn, S., Werner, C., Fee, D., Kelly, P., Doukas, M., Pfeffer, M., Webley, P., Cahill, C., & Schneider, D. (2013). Evaluation of Redoubt Volcano's sulfur dioxide emissions by the Ozone Monitoring Instrument. Journal of Volcanology and Geothermal Research, 259, 290-307.

McCormick, B. T., Edmonds, M., Mather, T. A., Campion, R., Hayer, C. S., Thomas, H. E., & Carn, S. A. (2013). Volcano monitoring applications of the Ozone Monitoring Instrument. Geological Society, London, Special Publications, 380(1), 259-
30   291.McCormick, B.T., M. Edmonds, T.A. Mather, and S.A. Carn (2012). First synoptic analysis of volcanic degassing in Papua New Guinea, Geochem. Geophys. Geosyst., 13(3), Q03008, doi:10.1029/2011GC003945.

Miller, T. P., & Casadevall, T. J. (2000). Volcanic ash hazards to aviation. Encyclopedia of volcanoes, 915-930.

Murphy, S. W., de Souza Filho, C. R., & Oppenheimer, C. (2011). Monitoring volcanic thermal anomalies from space: Size matters. Journal of Volcanology and Geothermal Research, 203(1), 48-61.

Atmospheric
Measurement
Techniques
Discussions

Prata, A. J. (2009). Satellite detection of hazardous volcanic clouds and the risk to global air traffic. Natural hazards, 51(2), 303-324.

Oommen, T., Baise, L. G., & Vogel, R. (2010). Validation and application of empirical liquefaction models. Journal of geotechnical and geoenvironmental engineering, 136(12), 1618-1633.

Oommen, T., Baise, L. G., & Vogel, R. M. (2011). Sampling bias and class imbalance in maximum-likelihood logistic regression. Mathematical Geosciences, 43(1), 99-120.

Rodríguez, J. D., Perez, A., & Lozano, J. A. (2010). Sensitivity analysis of k-fold cross validation in prediction error estimation. Pattern Analysis and Machine Intelligence, IEEE Transactions on, 32(3), 569-575.

Schneider, D. J., Dean, K., Dehn, J., Miller, T., & Kirianov, V. Y. (2000). Monitoring and analyses of volcanic activity using remote sensing data at the Alaska Volcano Observatory: case study for Kamchatka, Russia, December 1997. Remote Sensing of Active Volcanism, 65-85.

Siebert, L., Simkin, T., & Kimberly, P. (2011). Volcanoes of the World. Univ of California Press.

Self, S., Zhao, J. X., Holasek, R. E., Torres, R. C., & King, A. J. (1993). The atmospheric impact of the 1991 Mount Pinatubo eruption.

Sparks, R. S. J., Biggs, J., & Neuberg, J. W. (2012). Monitoring volcanoes. Science, 335(6074), 1310-1311.Telling, J.W, Flower, V.J.B., Carn, S.A., (2015). A multi-sensor satellite assessment of SO_2 emissions from the 2012-13 eruption of Tolbachik volcano, Kamchatka. Journal of Volcanology and Geothermal Research.

Witten, I. H., & Frank, E. (2005). Data Mining: Practical machine learning tools and techniques. Morgan Kaufmann.

Wright, R., Flynn, L., Garbeil, H., Harris, A., & Pilger, E. (2002). Automated volcanic eruption detection using MODIS. Remote sensing of environment, 82(1), 135-155.

Wright, R., Flynn, L. P., Garbeil, H., Harris, A. J., & Pilger, E. (2004). MODVOLC: near-real-time thermal monitoring of global volcanism. Journal of Volcanology and Geothermal Research, 135(1), 29-49.

Yang, K., Krotkov, N.A., Kruger, A.J., Carn, S.A.., Bhartia, P.K, & Levelt, P.F. (2007). Retrieval of large volcanic SO_2 columns from the Aura Ozone Monitoring Instrument: comparison and limitations. Journal of Geophysical Research D: Atmospheres, 112, doi: 10.1029/2007JD008825

Table 1: Characteristics of the methods incorporated in the development of an automatic classification technique

Method	Sample area size	Position	Correction technique
M1	4°×4°	Centred over the volcano	None applied
M2	2°×2°	Centred over the volcano	None applied
M3	2°×2°	Centred over the volcano	Assumes that the plume is predominantly confined to the M2 region and utilises the M1 region to define the background SO_2 level (Eq. 1).

5

10

15

20

25

Atmospheric
Measurement
Techniques
Discussions

Table 2: Test dataset of volcanic eruption dates and control dates (organized alphabetically by volcano)

Volcano	Location	Eruption Date	Control Date
Ambrym	Vanuatu	08/11/2006	31/03/2005
		23/05/2008	04/06/2008
Anatahan	Mariana Islands	06/01/2005	11/05/2009
		05/04/2005	16/06/2006
		17/03/2006	15/01/2007
		24/02/2007	22/11/2005
		27/11/2007	29/06/2005
Bagana	Papua New Guinea	17/03/2005	26/11/2007
		06/06/2005	14/06/2008
		09/01/2007	25/04/2005
		10/03/2007	23/10/2006
		20/05/2007	06/11/2006
		14/07/2007	01/07/2009
		23/08/2007	22/01/2006
		12/09/2007	26/12/2009
		06/10/2007	01/03/2009
Bezymianny	Kamchatka, Russia	10/05/2007	31/01/2005
		11/07/2008	22/05/2008
Chaitén	Chile	02/05/2008	11/12/2009
Dukono	Indonesia	25/05/2008	03/03/2006
		25/07/2008	02/10/2008
Fuego	Guatemala	27/12/2005	03/04/2008
Ibu	Indonesia	04/04/2008	16/07/2008
Kathala	Comoros	16/04/2005	07/07/2005
		24/11/2005	12/09/2006
		28/05/2006	17/10/2008
		12/01/2007	24/05/2009
Kelut	Indonesia	18/05/2006	21/02/2006
Manam	Papua New Guinea	27/01/2005	15/07/2005
		17/07/2006	25/02/2005
		05/10/2007	24/11/2008
		29/12/2007	07/08/2005
		11/05/2008	04/07/2008
Mayon	Philippines	17/08/2005	02/08/2006
		21/02/2006	27/03/2008
Merapi	Indonesia	07/03/2006	29/05/2008
		11/03/2006	31/03/2007

16

Atmospheric
Measurement
Techniques
Discussions

Open Access

EGU

Nyamuragira	DR Congo	27/11/2006	09/12/2007
		02/01/2010	11/05/2009
		06/11/2011	03/09/2008
		22/06/2014	31/08/2008
Nyiragongo	DR Congo	07/09/2005	22/06/2006
		10/10/2005	27/08/2005
		07/11/2005	08/03/2007
		01/01/2009	09/05/2009
Ol Doinyo Lengai	Tanzania	20/07/2005	20/07/2005
		30/03/2006	11/03/2008
Pagan	Mariana Islands	11/01/2007	24/06/2007
Piton de la Fournaise	Réunion	24/02/2005	01/02/2006
		20/07/2006	22/03/2007
		30/08/2006	13/11/2008
Popocatepetl	Mexico	06/04/2006	22/02/2006
		23/05/2006	27/08/2005
		11/04/2007	08/03/2007
		01/12/2007	09/05/2009
		22/02/2008	25/02/2005
		16/11/2008	11/03/2008
Rabaul	Papua New Guinea	07/10/2006	24/06/2007
		04/08/2007	01/02/2006
		22/08/2007	22/03/2007
Santa Ana	El Salvador	01/10/2005	13/11/2008
Santa Maria	Guatemala	26/10/2005	22/02/2006
SHV	Montserrat	20/05/2006	10/04/2009
		08/01/2007	12/03/2008
		29/07/2008	05/06/2007
		11/02/2010	02/04/2007
Soputan	Indonesia	19/04/2005	07/02/2005
		15/12/2006	10/05/2009
		15/12/2006	17/11/2008
		06/06/2008	20/12/2006
Tinakula	Solomon Islands	12/02/2006	03/02/2009
		22/09/2009	15/06/2009
		17/01/2010	05/10/2005
Tungurahua	Ecuador	14/07/2006	16/06/2005
		16/08/2006	31/12/2009
		10/01/2008	04/05/2009
		06/02/2008	11/02/2007
Turrialba	Costa Rica	06/01/2010	06/09/2005
		12/01/2012	04/08/2005

Atmospheric
Measurement
Techniques
Open Access
EGU
Discussions

Table 3: Average SO$_2$ column amounts (t) for volcanic and control events.

	Sample	Average SO$_2$ mass (tons)
Volcanic	**M1 (4°)**	2680
	M2 (2°)	1150
	M3 (Corrected)	680
Control	**M1 (4°)**	450
	M2 (2°)	170
	M3 (Corrected)	90

5

10

15

20

Atmospheric
Measurement
Techniques
Discussions

Table 4: Misclassified alerts identified in the initial logistic regression model

Sample (S)		Name	Date	Plume SO$_2$ Mass (tons)	Predicted Classification	Original Classification	Error Generation
C	1	Ambrym	31/03/2005	1040	Volcanic	Control	Persistent degassing
C	8	Bagana	26/11/2007	340	Volcanic	Control	Persistent degassing
C	10	Bagana	23/10/2006	?	Volcanic	Control	Missing data
C	24	Karthala	07/07/2005	?	Volcanic	Control	Missing data
C	29	Manam	15/07/2005	350	Volcanic	Control	Localised noise
C	32	Manam	07/08/2005	450	Volcanic	Control	Small Eruption
C	54	Popocatepetl	08/03/2007	600	Volcanic	Control	Ongoing eruption
C	57	Popocatepetl	11/03/2008	340	Volcanic	Control	Ongoing eruption
V	3	Anatahan	06/01/2005	230	Control	Volcanic	Diffuse plume
V	5	Anatahan	17/03/2006	120	Control	Volcanic	Drifting plume
V	13	Bagana	14/07/2007	320	Control	Volcanic	Diffuse plume
V	17	Bezymianny	10/05/2007	140	Control	Volcanic	Drifting plume
V	19	Chaiten	02/05/2008	250	Control	Volcanic	High noise
V	20	Dukono	25/05/2008	300	Control	Volcanic	Diffuse plume
V	21	Dukono	25/07/2008	270	Control	Volcanic	Drifting plume
V	23	Ibu	04/04/2008	210	Control	Volcanic	Diffuse plume
V	24	Karthala	16/04/2005	110	Control	Volcanic	Drifting plume
V	28	Kelut	18/05/2006	170	Control	Volcanic	Diffuse plume
V	32	Manam	29/12/2007	80	Control	Volcanic	Diffuse plume
V	33	Manam	11/05/2008	190	Control	Volcanic	Diffuse plume
V	34	Mayon	17/08/2005	120	Control	Volcanic	Drifting plume
V	43	Nyiragongo	10/10/2005	230	Control	Volcanic	Drifting plume
V	48	Pagan	11/01/2007	160	Control	Volcanic	Diffuse plume
V	53	Popocatepetl	23/05/2006	250	Control	Volcanic	Interfering signal
V	64	SHV	08/01/2007	240	Control	Volcanic	Drifting plume
V	67	Soputan	19/04/2005	169.9933	Control	Volcanic	Drifting plume

Atmospheric
Measurement
Techniques
Open Access
Discussions
EGU

Table 5: Locations and dates of volcanic and control 'eruptions' for validation dataset.

Volcano	Location	Eruption Date	Correct Classification (Y/N)		Control Date	Correct Classification (Y/N)	
			Original	Optimised		Original	Optimised
Ambrym	Vanuatu	01/05/2007	N	Y	12/12/2008	N	Y
Anatahan	Mariana Islands	29/05/2006	Y	Y	06/09/2005	Y	Y
Cleveland	Aleutian Islands	06/02/2006	Y	Y	17/05/2009	Y	Y
		23/05/2006	Y	Y	06/01/2008	Y	Y
		28/10/2006	N	N	28/02/2006	N	N
Colima	Mexico	24/04/2005	N	N	04/05/2009	Y	Y
Lascar	Chile	04/05/2005	N	N	11/02/2007	Y	Y
Lopevi	Vanuatu	21/04/2007	Y	Y	13/12/2006	Y	Y
Okmok	Aleutian Islands	12/07/2008	Y	Y	01/07/2008	Y	Y
Sierra Negra	Galápagos Islands	22/10/2005	Y	Y	04/08/2005	Y	Y
Soputan	Indonesia	25/10/2007	Y	Y	02/07/2008	Y	Y
Soufriere Hills	Montserrat	20/05/2006	N	N	24/08/2006	Y	Y

5

Table 6: Validation statistics generated through the assessment of the test data with three methods.

Validation Statistic	Original model	Optimised model	Optimised Threshold Model
Overall accuracy (%)	75	79.2	95
Volcanic Precision	0.8	1	1
Volcanic Recall	0.667	0.583	0.889
Control Precision	0.714	0.706	0.917
Control Recall	0.833	1	1
ROC	0.813	0.84	0.979
Threshold (P)	0.432	0.620	0.660

Atmospheric
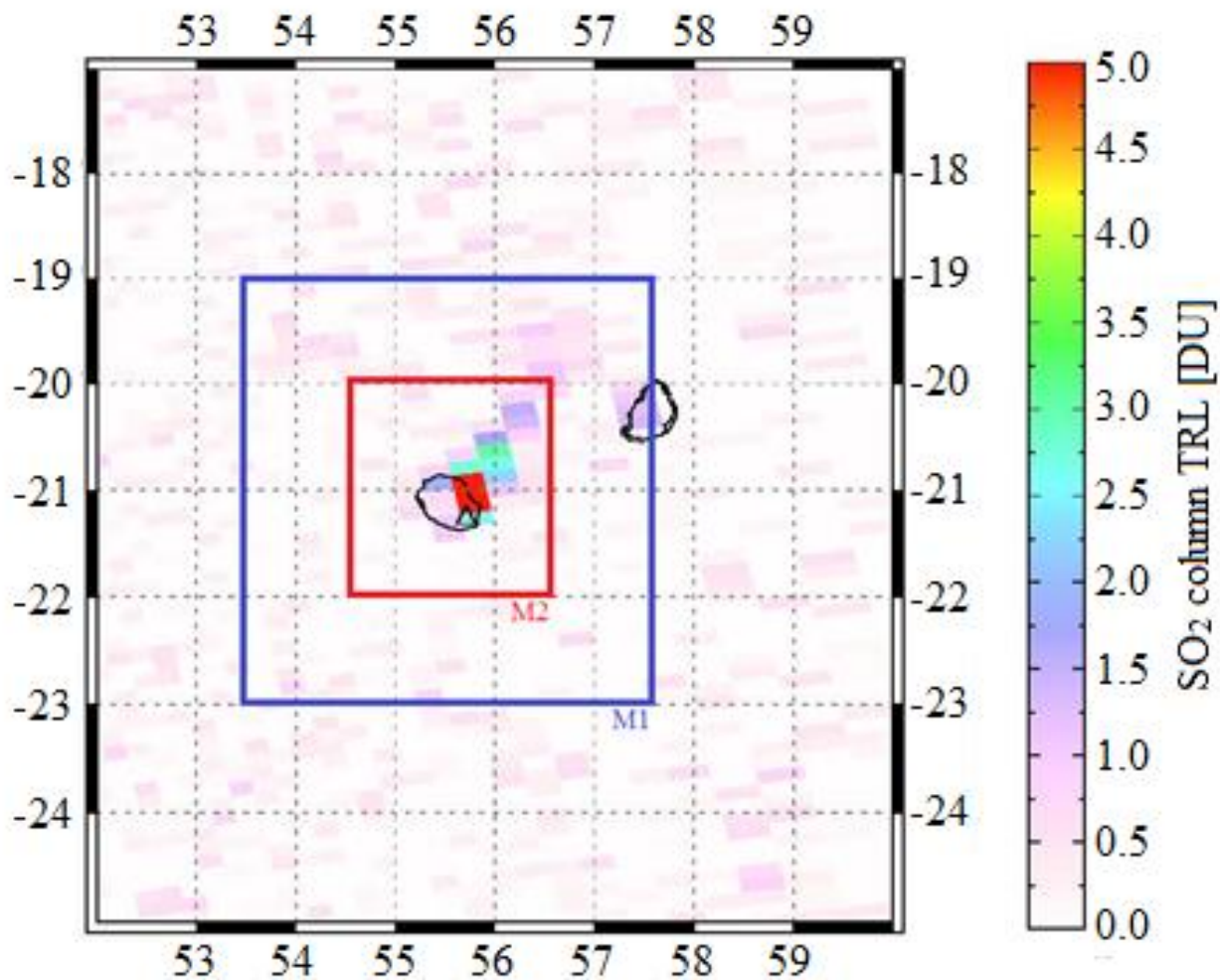Measurement
Techniques
Discussions

Figure 1: Analysis regions for Method 1 (M1) and Method 2 (M2) for an SO₂ plume detected by OMI at Piton de la Fournaise, Réunion on the 24th February 2010.

Atmospheric
Measurement
Techniques
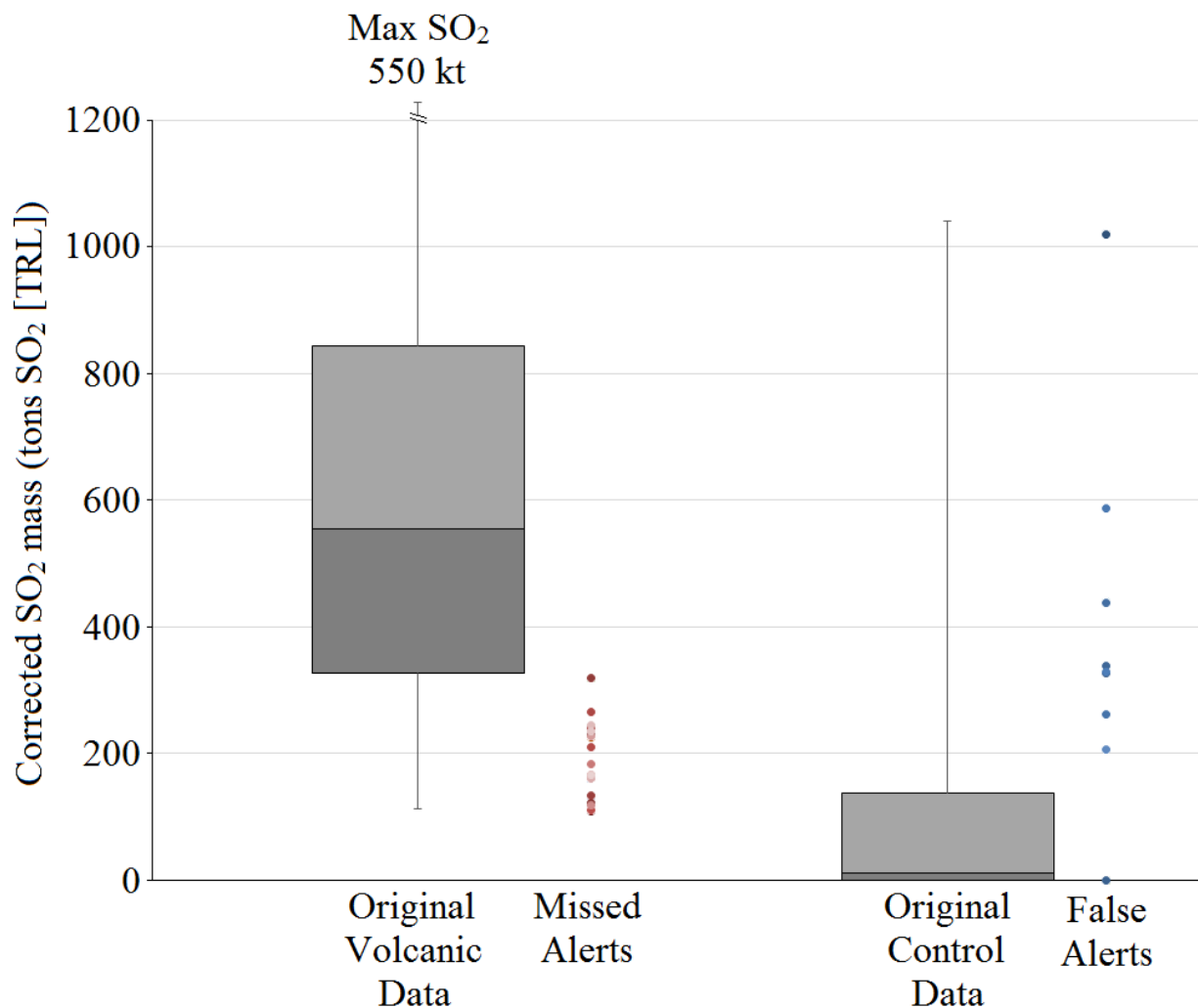Discussions

Open Access

EGU

Figure 2: Box and whisker plots displaying the spread and distribution of volcanic and control data with lines indicating upper and lower quartiles of the data and the remainder represented by the box region. Additional data points indicate the individual missed alerts in the volcanic data and false alerts in the control data detailed in Table 4.
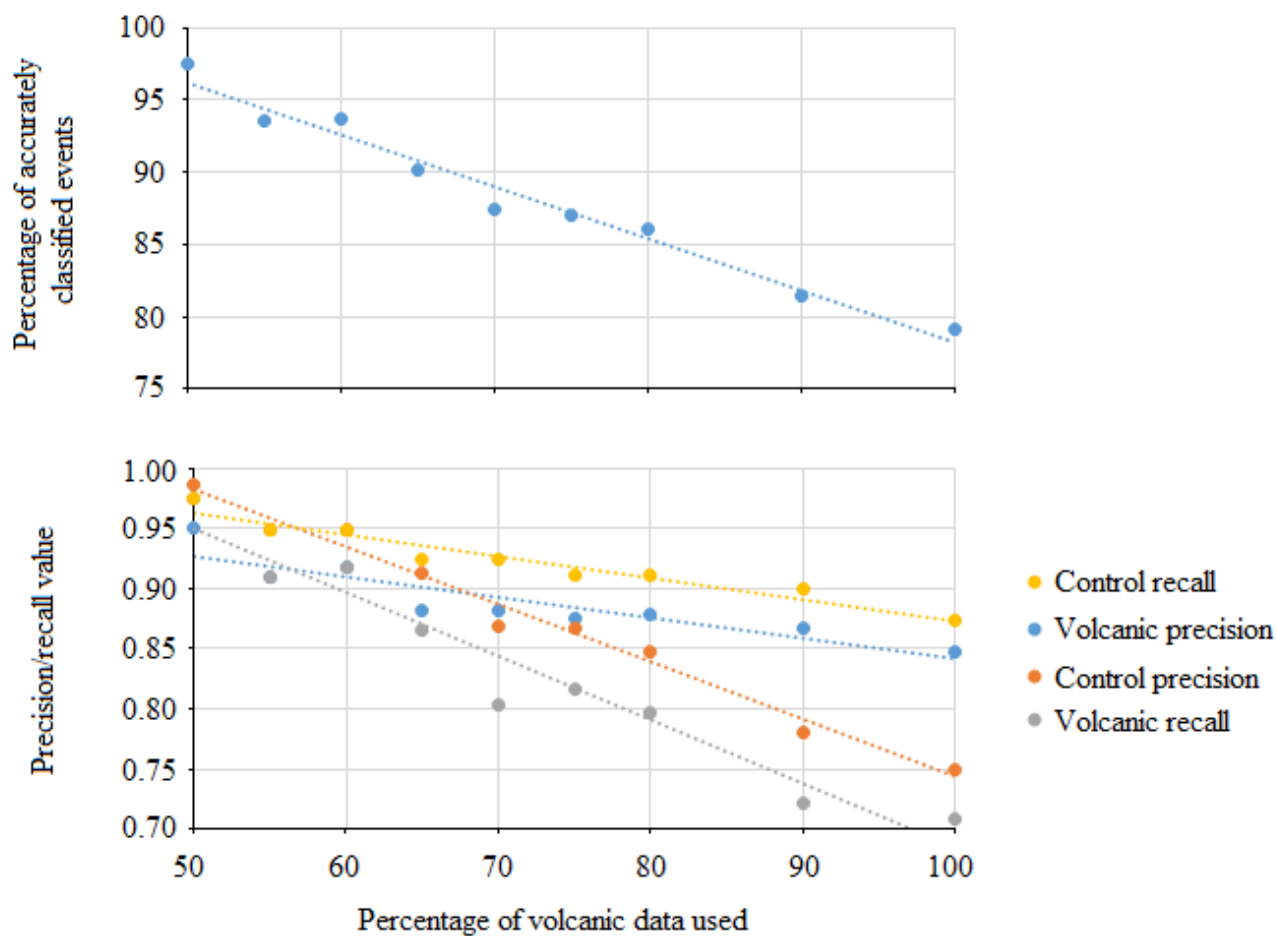
Atmospheric
Measurement
Techniques

Open Access

EGU

Discussions

Figure 3: Result of the application of a threshold SO₂ loading to the volcanic dataset on; a. accurately classified events and b. the precision (no false alerts) and recall (no missed alerts) values for both the volcanic and control datasets.

Atmospheric
Measurement
Techniques
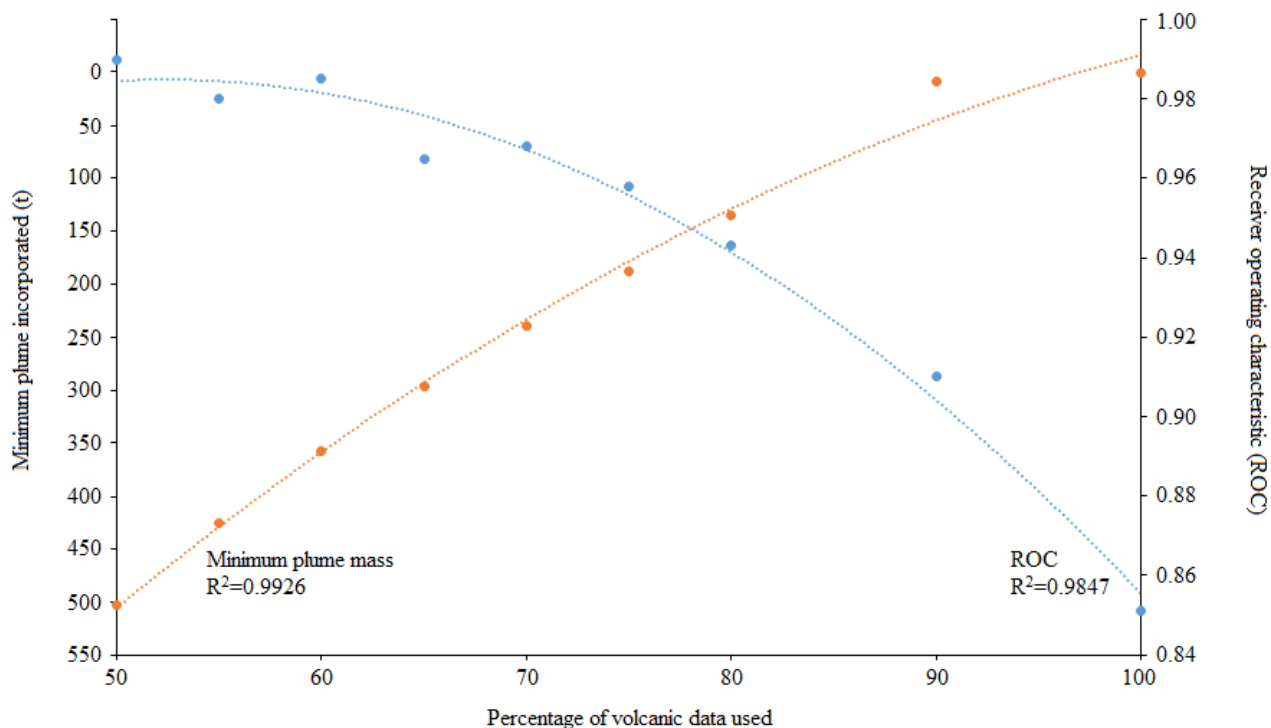Discussions

Open Access

Figure 4: The effect of proportional removal of lowest data points on minimum incorporated SO₂ mass from the volcanic dataset and the ROC (receiver operator characteristic) statistic of each model where ROC = 1 implies all events correctly classified.